Environ. Sci. Technol. **2001**, *35,* 3130−3138

Formation of Aerosol Particles from Reactions of Secondary and Tertiary Alkylamines: Characterization by Aerosol Time-of-Flight Mass Spectrometry

STEFANIA ANGELINO, DAVID T. SUESS, AND KIMBERLY A. PRATHER*

Department of Chemistry, University of California, Riverside, California 92521-0403

In ambient field studies conducted with aerosol time-of-flight mass spectrometry (ATOFMS), individual particle mass spectra commonly contain ion peaks at mass/charge (*m*/*z*) 86, 101, 102, and 118. Particles with mass spectra containing these peaks show a strong correlation with high relative humidity and low temperatures. In an effort to identify these peaks, a series of smog chamber studies were conducted probing the chemistry of secondary and tertiary alkylamines. Specifically, in separate studies, trimethylamine, di- and triethylamine, and di- and tripropylamine were reacted in a 1 m^3 Teflon outdoor smog chamber with naturally occurring levels of gas phase oxidants in ambient air. The aerodynamic sizes and individual mass spectra of the resulting aerosol particles were acquired continuously using aerosol time-of-flight mass spectrometry (ATOFMS). Both oxidation and acid−base reactions between amines and acids commonly present in the atmosphere (i.e., nitric and sulfuric acid) appear to play roles in the formation and chemistry of organic nitrogen-containing particle phase species. Ion peaks in the individual particle mass spectra indicate the presence of alkyl ammonium salts, as well as other tentatively identified organic *N*-containing compounds formed by oxidation processes. Also, for the first time, tertiary alkylamine-*N*-oxides have been identified as alkylamine oxidation products in the aerosol particle phase. Smog chamber reactions involving triethylamine produce ATOFMS mass spectra with similar ion peak combinations as those observed in the spectra of particles commonly detected in ambient and vehicular source characterization studies. The results of this study suggest that amine chemistry involving gas-to-particle conversion and photooxidation processes may play a significant role in particle formation in regions with high amine concentrations.

Introduction

Low molecular weight aliphatic amines are emitted by a variety of widespread anthropogenic and biogenic sources, constituting an important class of environmental pollutants due to their toxic and odorous properties. A number of short chain alkylamines have been detected in industrial emissions and car exhaust (*1*−*3*), as well as air samples from cattle feedlots (*4*, *5*), waste incinerators, and sewage treatment plants (*6*). Contributions from these sources most likely lead to ambient background levels of aliphatic amines; however, few studies have addressed their chemistry and evolution in the atmosphere.

A limited number of studies have investigated the atmospheric reaction processes of amines. Typical estimated atmospheric lifetimes for amines are on the order of a few hours up to several tens of hours. Aliphatic amines absorb light at wavelengths below 250 nm and thus do not undergo photolysis in the troposphere. Like most organic compounds, amines become transformed through reactions with oxidants such as hydroxyl radicals and ozone (*1*). The reactivity of alkylamines received some attention in the 1970s when the carcinogenicity of their nitrosation products (nitrosamines) (*7*, *8*) was discovered. In particular, gas-phase secondary amine photooxidation processes were studied in environmental chamber reactions with FTIR detection (*9*). However, after it was shown that nitrosamines rapidly undergo photolysis in sunlight, and thus do not accumulate in the atmosphere (*10*), the interest toward alkylamines decreased. In studies of gas-phase amine photooxidation processes, as reported by Finlayson-Pitts and Pitts, a significant fraction of the reacted parent amine remains unaccounted for in the identified gas-phase products (*11*). In general, the current understanding of the gas-phase chemistry of amines is far more developed than that for amines in the particle phase. In fact, to our knowledge, just one paper reports a light backscattering increase during di- and triethylamine smog chamber photooxidation, indicating secondary aerosol formation from alkylamines (*9*).

Over the past decade, a number of real-time single particle mass spectrometry (RTSPMS) techniques have been developed, offering new opportunities for studying aerosol particulate matter (*12*). Among RTSPMS techniques, aerosol time-of-flight mass spectrometry (ATOFMS) can be used to determine in real-time both the size and chemical composition of individual particles (*13*, *14*). To date, ATOFMS has been used primarily for studying atmospheric aerosols and performing source characterization studies. In these studies, interpretation of the mass spectra of inorganic single particle types (e.g., sea salt, dust, soil) is relatively straightforward; however, interpretation of the organic aerosol particle mass spectra is a much more challenging task. This is due to both the complexity of the organic matrix (i.e., a single particle may contain hundreds of different organic species) and the fragmentation processes that occur during the laser desorption/ionization (LDI) process.

Smog chamber studies can provide a bridge between the data acquired in field studies and controlled laboratory measurements by monitoring organic aerosol formation processes in a less complex environment than the atmosphere. Using this approach, mass spectral interpretation is greatly facilitated by knowing the particular reactive organic gas (ROG) that is the precursor of particle formation. Identification of all reaction products in the particle phase is not the goal of these studies. Instead, a more realistic goal is to make "reasonable" hypotheses for some of the major components that will allow particular particle types detected in ambient air to be related to certain classes of emitted compounds, which potentially can be associated with the primary sources.

Thus, the major goals of the present work are 3-fold: (i) test the utility of using ATOFMS as an on-line detector for atmospheric reactions simulated in a smog chamber,

* Corresponding author phone: (909) 787 3143; fax: (909) 787 4713; e-mail: prather@citrus.ucr.edu.

10.1021/es0015444 CCC: $20.00
Published on Web 06/22/2001

(ii) investigate the mass spectra of secondary and tertiary alkylamines, alkyl ammonium salts, and particles formed in the presence of alkylamines and ambient gas phase oxidants, and (iii) use the results of the laboratory investigations to identify the species producing commonly observed ion peaks in ambient particle mass spectra.

Experimental Section

Materials. The amine standards used in this study include trimethylamine (TMA, 20% solution in methanol), diethylamine (DEA), triethylamine (TEA), dipropylamine (DPA), and tripropylamine (TPA). The standards were purchased from Aldrich (Milwaukee, WI) and used without purification. Deuterated triethylamine (TEA-d_{15}, 98%) was obtained from Cambridge Isotope Laboratories, Inc. (Andover, MA).

ATOFMS Alkylamine Analysis. Aerosol time-of-flight mass spectrometry (ATOFMS) has been described in detail previously (*13*−*15*). For the experiments reported here, both the laboratory-based (*13*, *14*) ATOFMS and the transportable dual ion version of the instrument (*15*) were used. ATOFMS is capable of in-situ analysis of polydisperse aerosol samples in real time, simultaneously providing precise aerodynamic particle size and chemical information on individual particles. The interface consists of a convergent nozzle, followed by two and three differentially pumped regions in the transportable and lab-based version of the instrument, respectively. Pressures are successively lowered in each region to reach an operating pressure in the time-of-flight mass spectrometer of 10^{-7} Torr. Particles are collimated into a narrow beam as they move through the skimmers separating the differentially pumped regions. Each particle then passes through a light scattering region, where it successively encounters the light from two continuous wave diode lasers. The light scattered from a particle intersecting the first laser is detected by a photomultiplier tube, which initiates a timer in an electronic timing/logic circuit. At a fixed distance further into the instrument, the particle crosses a second laser beam, orthogonally oriented with respect to both the particle beam and the first laser beam, which results in a second scatter pulse that halts the counting in the timing/logic circuit. The measured particle transit time between the two scattering signals is used to determine the velocity of each particle traveling directly through the center of the light scattering region and thus toward the ion source of the mass spectrometer. The velocity is used to obtain the aerodynamic diameter (d_a) of the particle, using a calibration curve obtained using polystyrene latex sphere (PSL) suspensions of known sizes in the range between 0.2 and 2.5 μm. The measured transit time is also used to synchronize the firing of a frequency quadrupled (266 nm) Nd:YAG laser. This laser pulse desorbs and ionizes molecules from the particle in the ion source region of a reflectron time-of-flight mass spectrometer. Positive and negative ion mass spectra are acquired separately by changing the applied voltages on the source and reflectron regions in the laboratory-based ATOFMS. The transportable ATOFMS, equipped with a dual co-linear time-of-flight mass spectrometer, acquires both positive and negative ion mass spectra simultaneously. The resulting mass spectra of the ions produced from each particle are recorded and stored along with the particle transit time between the two scattering lasers.

To investigate the laser desorption/ionization (LDI) ATOFMS fragmentation patterns of standard (unreacted) alkylamines, two particle generation techniques were employed. First, MilliQ aqueous standard solutions were nebulized using a home-built Collison atomizer. The particles obtained were characterized by a broad size distribution covering the entire size range detected by the ATOFMS (0.2 μm < d_a < 3 μm) with a maximum at approximately 1.5 μm. Mass spectra were obtained for both wet particles (directly introduced into the ATOFMS without a drier) and dry particles (sent through a silica gel drier). In the second type of particle generation experiment, particles were formed directly by acid−base reactions and sent directly into the ATOFMS for analysis. Aliquots of 1 mL of alkylamine and 1 mL of acid (nitric, formic, or acetic) were introduced into a 5-L glass bottle, instantaneously producing particles containing the respective alkyl ammonium salts (nitrate, formate, or acetate). In these experiments, the particle size distributions measured by the ATOFMS were quite broad, with aerodynamic sizes primarily between 0.2 and 1.5 μm and a maximum at approximately 0.8 μm.

TABLE 1. Sequence of the Smog-Chamber Experiments Performed and Relative Conditions

day	amine	NO_x (ppb)	O_3 (ppb)	RH %	other conditions
7/16/99	TEA	75	15	56	
7/25/99	DEA	62	28	57	
8/08/99	TPA	32	25	51	
8/11/99	DPA	51	30	58	
8/19/99	TMA	48	31	55	
8/02/99	TEA	98	12	20	used a silica gel drier
8/21/99	DEA			20	clean air + CH_3NO_2 (~1 ppm)
8/18/99	DEA	65	26	62	dark
9/03/99	DEA			0.1	clean air + CH_3NO_2 (~1 ppm)
9/29/99	TEA-d_{15}	74	12	52	

Smog Chamber Experiments. Secondary organic aerosol (SOA) particles were generated by simulating atmospheric reactions in a 1 m^3 Teflon outdoor chamber. Wall losses, probably significant in such a small bag, were not a concern here given the aim of this study. The SOAs produced by the reactions were analyzed continuously using the ATOFMS connected directly to the chamber using a 3/8 in. i.d. copper sampling line. Limited by optical detection, the lower particle size detection limit in these experiments was approximately 0.2 μm. After several hours (typically 3−5, depending on the amine and/or the daily ambient gas-phase concentrations), particles with aerodynamic diameters ranging from 0.2 to 0.4 μm were detected.

Experiments were conducted in July−September 1999 at the University of California, Riverside. The procedure consisted of filling the bag in the morning with particle-free ambient air with gas phase concentrations typical of Riverside summer conditions (see Table 1), adding a measured volume of liquid-phase amine to produce a concentration of approximately 0.5 ppm, and exposing the contents to sunlight. The amines were introduced by flowing a stream of air through the inlet and outlet ports of a round-bottom flask containing the desired amine directly into the smog chamber. A HEPA capsule filter (Pall Gelman Laboratory) was used to obtain particle-free ambient air for the experiments. The HEPA filter was tested prior to each experiment using a scanning mobility particle sizing (SMPS, TSI Inc., St. Paul, Minnesota) system and the ATOFMS by connecting the filter to the inlet of the sampling line and measuring the particle counts. The SMPS showed the filter effectively removed particles between 10 nm and 0.6 μm. The ATOFMS indicated that larger particles (d_a 0.2−3 μm) were also removed. No measurement was made on particles below 10 nm, and thus it is possible that sub-10 nm particles were introduced into the chamber.

Measurements of gas-phase species concentrations were made with a number of instruments. Atmospheric NO_x concentrations were measured using a model 42C Trace Level Chemiluminescence NO−NO_2−NO_x analyzer (Thermo Environmental Instruments Inc., Franklin, MA) calibrated with

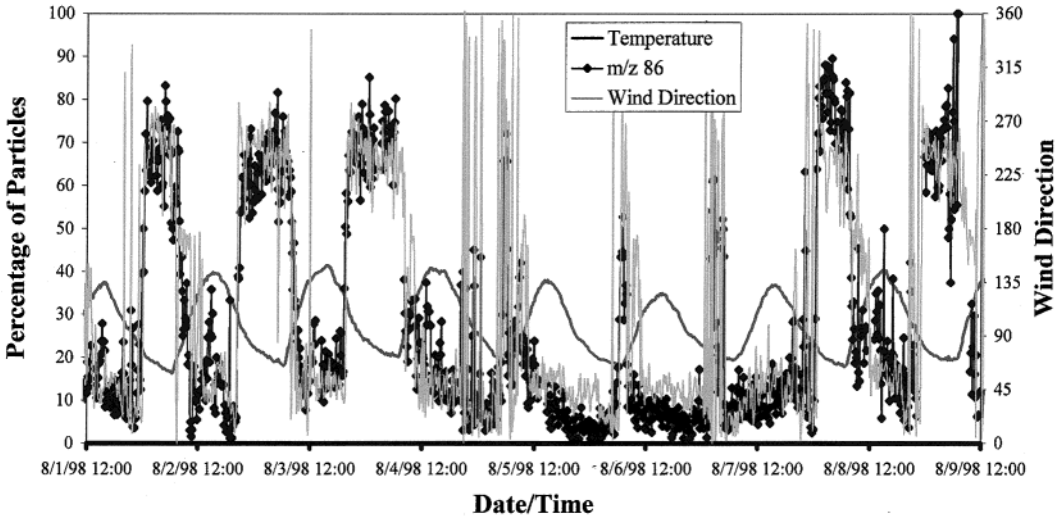

FIGURE 1. Temporal profile showing the percentage of particles with mass spectra containing an ion peak at *m/z* 86 sampled alongside a freeway in Riverside, CA, in August of 1998. Wind direction of 270° was blowing directly from freeway toward sampling site.

a Series 100 computerized multi-gas calibrator (Environics, Tolland, CT). O_3 concentrations were measured using a model 1003 AH ozone meter (Dasibi Environmental Corp., Glendale, CA). Relative humidity was determined using a digital hygrometer-thermometer (Fisher Scientific, Tustin, CA).

A number of control experiments were performed. The sequence of experiments and relevant conditions are reported in Table 1. One control experiment involved filling the Teflon bag with particle-free air from an air purification system equipped with an activated charcoal cartridge for organic compound removal, a CP blend media (Purafil Inc., Doraville, GA) cartridge for NO_x removal, and a silica gel drier. In this case, radicals were produced by the photolysis of methyl-nitrite (CH_3ONO) at wavelengths above 300 nm. To obtain an initial CH_3ONO concentration of approximately 1 ppmv, 0.5 Torr CH_3ONO was added to the chamber. Other experiments were carried out in the dark or at low relative humidity.

Results and Discussion

Ambient Observations. In previous field studies conducted with ATOFMS, as well as a vehicular exhaust source characterization study (*16*), particles containing ion peaks at mass/charge (*m*/*z*) 86, 101, 102, and 118 have been observed. The temporal profiles for particles with mass spectra containing these peaks exhibit similar trends, although in general, fewer contain *m*/*z* 101, 102, and 118. The most consistently observed peak in the mass spectrum occurs at *m*/*z* 86. On the basis of laser power dependence studies, it appears that species producing the higher mass peaks fragment to produce *m*/*z* 86.

Figure 1 shows the temporal evolution of the percentage of particles with mass spectra containing *m*/*z* 86 sampled within 20 ft of a freeway in Riverside, CA, during August 1998. Strong diurnal variations were evident. In general, during this study, the percentage of particles with mass spectra containing *m*/*z* 86 increased with decreasing temperature and increasing RH. In addition, a strong correlation between the percentage of particles with mass spectra containing *m*/*z* 86 and the wind direction was evident. When the wind was blowing directly from the freeway (~270°) toward the sampling site, relatively high percentages of single particle mass spectra with these peaks were observed. In contrast, when the wind blew in the opposite direction, fewer particle mass spectra with these peaks were detected. In general, the highest percentage of particle mass spectra with *m*/*z* 86 were detected when the wind blew from the freeway toward the sampling site, and the temperature was low and relative humidity was high. However, there were time periods (i.e., 8/4/98) when the temperature was relatively high (and the RH was low) and the wind was blowing from the freeway toward the sampling site that bursts of these particles were observed. In general, over the course of this study, there was a constant background of particles with mass spectra containing *m*/*z* 86. The strong correlations with wind direction suggest these species are associated with fresh mobile emissions. It is important to note that the Chino dairy area is located approximately 15 miles upwind of the freeway, and thus, when the wind shifted toward the sampling site, it also brought contributions from the dairy area. However, the observed instantaneous changes in the percentage of particles containing *m*/*z* 86 with changing wind direction suggest these species are emitted from a closely located source and thus most likely produced by vehicles traveling on the freeway. This is consistent with previous source characterization studies of mobile emissions that have also shown single particle mass spectra with peaks at *m*/*z* 86, 101, and 102 [16].

A similar temporal profile for the number of particles with mass spectra containing *m*/*z* 86 sampled in Atlanta, GA, in January 1999 during the EPA SuperSite experiment is shown in Figure 2. During this study, ATOFMS data were acquired continuously over a month long period. Similar to the data shown in Figure 1, during the four-day period shown, there were distinct relationships between temperature, relative humidity, and the number of particle mass spectra containing *m*/*z* 86. In both Figures 1 and 2, the relationship between relative humidity and temperature and the diurnal variations of particle mass spectra containing *m*/*z* 86 is similar to that of ammonium nitrate in ambient particles (*17*). The observed correlations between particles with mass spectra containing *m*/*z* 86 and temperature and relative humidity indicate the species producing these peaks are semivolatile in nature. These observations as well as results from a mobile source characterization study inspired us to perform lab studies in an effort to identify the species responsible for the described combination of peaks at *m*/*z* 86, 101, 102, and 118. Amines were initially selected for study based on the distinct mass spectral fragmentation patterns (*18*). Contributions of aliphatic amines to organic aerosol particle formation have not been previously investigated, although it is highly probable that reactions occur between amines and acids present in the atmosphere. Such reactions would produce the alkyl ammonium salts in direct analogy to the reactions that occur between ammonia and gas-phase acids. Moreover, like most

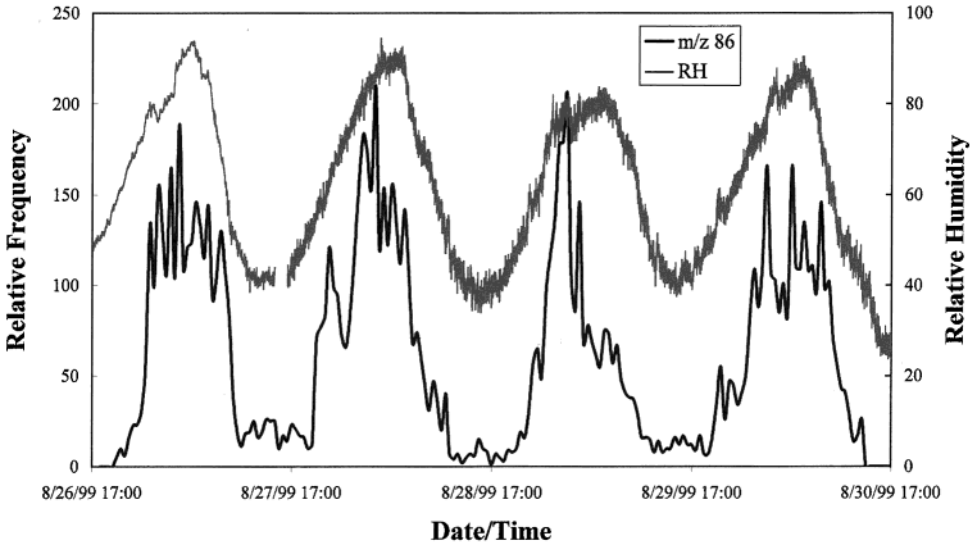

FIGURE 2. Temporal profile showing the frequency of individual particles with mass spectra containing an ion peak at *m/z* 86 sampled in Atlanta, GA, during the 1999 EPA Supersite experiment.

organic compounds present in the atmosphere, amines may also react with OH, NO_3, NO_2, and O_3, with the OH radical reaction most likely being the most significant atmospheric loss process. If the products of these reactions have lower vapor pressures than the parent amine, or basic properties, they also may contribute to particle formation together with the alkyl ammonium salts.

Mass Spectral Interpretation. The current knowledge of laser desorption/ionization (LDI) processes is still relatively limited. However, the typical features in the resulting mass spectra strongly depend on the operating conditions of the laser (i.e., wavelength, power, beam homogeneity). Moreover, when probing a particle with a high energy laser pulse, there is the possibility of rearrangements and/or reactions of the particle constituents in the laser plume. Therefore, understanding the complexity of ion formation processes, in particular when analyzing organic substances, requires detailed studies of the fragmentation patterns for the chemical class of interest under the same experimental conditions (*19*). In this study, reaction products are proposed that have not been identified before in the particle phase. Therefore, it is necessary to prove that these species actually were present in the particles and not just formed in the laser desorption plume from ion−molecule reactions of the parent amine. To this end, a preliminary investigation was carried out to characterize the behavior of amine compounds during ATOFMS LDI analysis. The ATOFMS results obtained for alkylamine aqueous standard solution droplets and the respective alkyl ammonium salts are described in the following section.

Standard Amines and Alkyl-Ammonium Salts ATOFMS Mass Spectral Characteristics. *Alkylamine Aqueous Standard Solutions.* Standard solutions containing trimethylamine, di- and triethylamine, and di- and tripropylamine were nebulized into the ATOFMS. The ATOFMS LDI mass spectra of the resulting particles are comparable to those obtained in both chemical ionization (*19*, *20*) and multiphoton ionization (*21*, *22*) studies reported in the literature. Representative mass spectra for each of the compounds studied are shown in Figure 3.

Aliphatic amines possess very low ionization potentials. However, the presence of the amine leads to cleavage reaction initiation in such a powerful way that the molecular ion abundance in the electron impact mass spectrum is usually negligible. In general, the most important primary fragmentation process occurring for aliphatic amines involves the

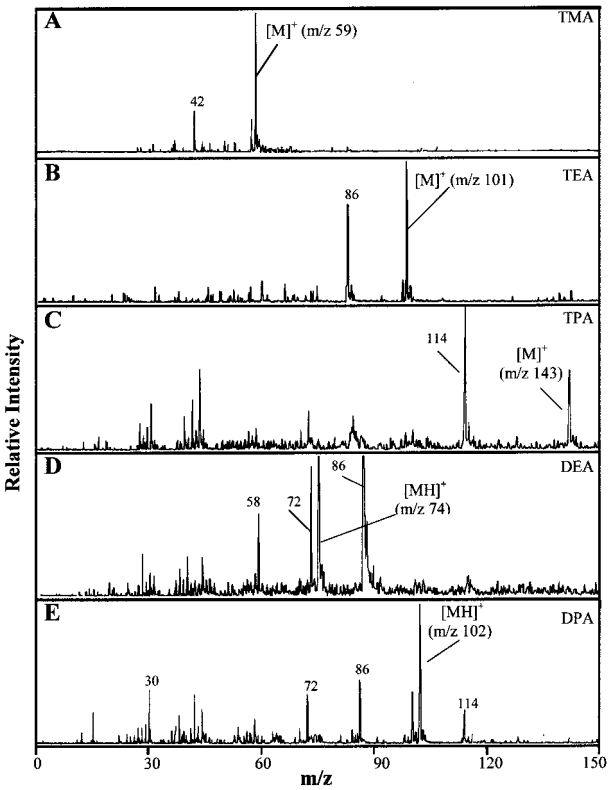

FIGURE 3. Representative mass spectra for individual alklyamine particles generated from aqueous standard solutions. (A) trimethylamine (TMA), (B) triethylamine (TEA), (C) tripropylamine (TPA), (D) diethylamine (DEA), and (E) dipropylamine (DPA).

removal of one of the electrons from the lone pair on N and cleavage of the C−C bond α to the nitrogen, with loss of the heavier alkyl group favored. This cleavage explains the presence of the fragments at *m/z* 58 $[C_2H_5NH{=}CH_2]^+$, 72 $[C_3H_7NH{=}CH_2]^+$, 86 $[(C_2H_5)_2N{=}CH_2]^+$, and 114 $[(C_3H_7)_2N{=}CH_2]^+$ in the mass spectra of DEA, DPA, TEA, and TPA, respectively. Other processes may also occur to a lesser extent, leading to smaller fragments, such as the signal at *m/z* 30 $[CH_2{=}NH_2]^+$ in many of the alkylamine mass spectra.

As shown in Figure 3A−C, ATOFMS analysis of trialkylamines produces relatively simple spectra with the most abundant signals at $[M]^+$ at *m/z* 59, 101, and 143 for TMA,

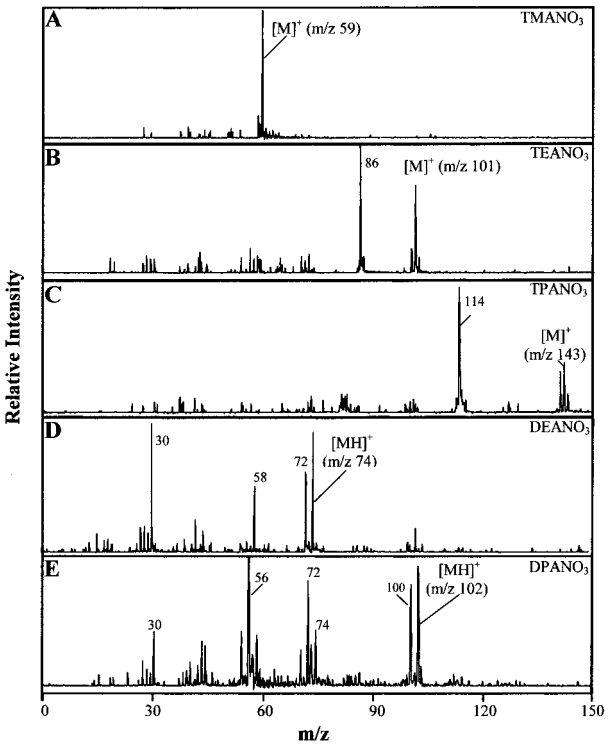

FIGURE 4. Representative positive ion single particle mass spectra obtained for alkyl ammonium nitrate particles. (A) trimethyl ammonium nitrate, (B) triethyl ammonium nitrate, (C) tripropylammonium nitrate, (D) diethylammonium nitrate, and (E) dipropylammonium nitrate.

TEA, and TPA, respectively. In addition, a major fragment occurs for TEA and TPA at m/z 86 and 114, resulting from loss of a methyl and ethyl group, respectively, leading to formation of an immonium ion, $[R_2N{=}CH_2]^+$, as discussed above. None of the standard amines analyzed produced negative ion mass spectra.

In contrast, the mass spectra for the dialkylamines (DEA and DPA), Figure 3D,E, obtained under the same conditions are more complex. In addition to the protonated, $[MH]^+$, and unprotonated, $[M-H]^+$, molecular ion, DEA and DPA particle mass spectra also show a signal at $[(M-1)+14]^+$ at m/z 86 and 114, respectively. One possible explanation for these peaks is the high concentration of amine in the ion plume, both in the ionized/fragmented and neutral forms, which leads to ion−molecule reactions. Specifically, the reaction between the fragment of the general structure $[C_nH_{n+1}NH{=}CH_2]^+$ and a neutral molecule of dialkylamine could give rise to the observed signal as shown here for DEA:

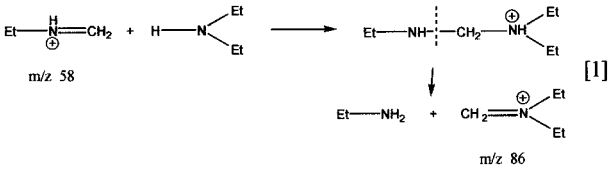

Alkyl Ammonium Salts. In this set of experiments, as described in Experimental Section, particles were formed by acid−base reactions. Nitric, formic, and acetic acids were used, representing both inorganic and organic carboxylic acids commonly found in ambient air. Figure 4 shows examples of representative ATOFMS single particle mass spectra for alkyl ammonium nitrate particles formed by reactions of nitric acid and each amine. In general, the peaks observed in the alkyl ammonium salts are very similar to those observed in the mass spectra of each respective amine (Figure 3). In direct analogy to the standard amine spectra, the mass spectra of trialkyl ammonium salts, organic and inorganic, and dialkyl ammonium organic salts contain $[M]^+$ (Figures 4A−C) for the tertiary amines (TMA, TEA, TPA) and $[MH]^+$ for the secondary amines (DEA, DPA) (Figure 4D,E). Although not as common as with the standard amines, dialkyl ammonium nitrates occasionally produce the $[(M-1)+14]^+$ signal described in the previous paragraph. In the dialkyl ammonium organic salt mass spectra, more extensive fragmentation is observed at lower m/z ratios. This extra fragmentation may be due to stronger absorption by the salts of the ultraviolet radiation.

Summary of Alkylamine and Alkyl Ammonium Salt Standard Particle Mass Spectra. The ion peaks at m/z 86, 101, and 102 were observed in the spectra of a number of the amines studied. Specifically, both the standard amines and alkyl ammonium salts of TEA and DEA can account for the peak at m/z 86. In fact, in previous ATOFMS studies, a number of amines have been shown to produce the ion peak at m/z 86, suggesting this ion peak might be a good general marker for amine compounds (*19*). However, to use m/z 86 as a general marker for amines in ambient studies, other ion peaks consistent with amines must be present in the same single particle positive and negative ion mass spectra. Particle mass spectra of both TEA and $TEANO_3$ contained the peak at m/z 101. The ion peak at m/z 102 was observed for TEA, DPA, and $TEANO_3$, and $DPANO_3$. However, none of the amine standards or salts produced the peak observed at m/z 118 observed in ambient studies. Since it was not a significant peak in particles produced in the dynamometer study, it appears that this peak is produced by reactions of mobile emission particles that occur in the atmosphere. In an effort to simulate those reactions and produce particles with m/z 118, the series of smog chamber reactions described in the next section were performed.

Smog Chamber Reactions of Alkylamines. To study aerosol formation in the presence of short chain alkylamines, ATOFMS was employed as an on-line detector for smog chamber experiments. This experiment differed from traditional smog chamber studies by using real ambient air as opposed to the standard configurations that use air with relatively high levels of added oxidants. The high sensitivity of the ATOFMS system allows one to monitor the resulting low particle product concentrations. These studies were performed using ambient concentration levels of gas-phase species (e.g., NO_x, O_3) to make the reaction processes occurring in the smog chamber more representative of processes that occur in the atmosphere. All five amines produced aerosol particles during the smog chamber reactions performed according to the procedure described in Experimental Section.

The aerodynamic diameters of the particles detected by ATOFMS in all the alkylamine reactions were in the 0.2−0.6 μm size range. Representative mass spectra for particles obtained from the various amine smog chamber reactions are shown in Figure 5. The spectra for these particles typically exhibit similar features in the low mass range, due to analogous fragmentation patterns for most of the compounds formed in the alkylamine reactions. Differences are found instead at higher masses and can be attributed to the oxidation products characteristic of each amine. All negative ion mass spectra reveal the presence of nitrates and, less frequently, sulfates, as well as signals from organic compounds.

Tertiary Alkylamine Reactions−Positive Ion Mass Spectra. When the parent compound leading to particle formation is a tertiary alkylamine, the mass spectra obtained are relatively simplistic. As shown in Figures 5A−C, the new feature that was not observed in the amine standard or alkyl ammonium salt particle mass spectra is the ion signal at $[M+17]^+$, m/z

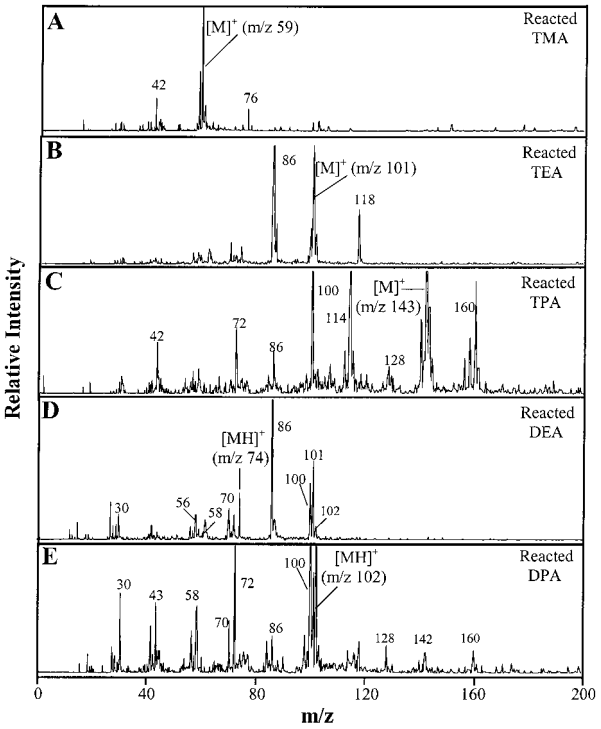

FIGURE 5. Representative positive ion single particle mass spectra obtained from alkylamine reactions in a smog chamber. Reactant: (A) TMA, (B) TEA, (C) TPA, (D) DEA, and (E) DPA. Most probable assignments for major ion peaks: (A) *m/z* 58, 59, 60, assigned as $[M-H]^+$, $[M]^+$, and $[MH]^+$, respectively, and *m/z* 76 $[TMAOH]^+$; (B) *m/z* 86 $[(C_2H_5)_2N{=}CH_2]^+$, *m/z* 100, 101, 102, $[M-H]^+$, $[M]^+$, and $[MH]^+$, respectively, and *m/z* 118 $[TEAOH]^+$; (C) *m/z* 72 $[C_4H_9NH]^+$, *m/z* 100 $[(C_3H_7)_2N]^+$, *m/z* 114 $[(C_3H_7)_2N{=}CH_2]^+$, *m/z* 143 $[M]^+$, 144 $[MH]^+$, and *m/z* 160 $[TPAOH]^+$; (D) and (E) see text.

76 for TMA, *m/z* 118 for TEA, and *m/z* 160 for TPA. Most of the other signals were also observed in the standard amine and alkyl ammonium salt particle mass spectra. Specifically, for the TMA, TEA, and TPA reactions, the base signal is always $[M]^+$ at *m/z* 59, 101, and 143, respectively. In addition, ion peaks resulting from alkyl losses are also observed at *m/z* 86 $[(C_2H_5)_2N{=}CH_2]^+$ and 114 $[(C_3H_7)_2N{=}CH_2]^+$. These peaks are coupled with two less intense signals resulting from protonation and deprotonation of the molecular ion $[M]^+$ of the parent amine. About 20−30% of the particles formed by TMA reactions also have signals at *m/z* 62, 72, and 91. On the basis of gas-phase amine reaction products reported in the literature (*1*, *5*, *9*), these signals can be tentatively assigned to $[(CH_3)_2NHOH]^+$, $[CH_2{=}N(CH_3)CHO]^+$, and $[(CH_3)_2NHNO_2]^+$, respectively. Particles with a signal at *m/z* 91 in the positive ion spectrum also show a corresponding peak in the negative ion mass spectrum at *m/z* −90.

Secondary Alkylamine Reactions−Positive Ion Mass Spectra. Figure 5D,E show the mass spectra of particles generated in the dialkylamine reactions. In comparison to the mass spectra for the tertiary amines (Figure 5A−C), more ion signals are observed at *m/z* values higher than the molecular ion $[M]^+$. This is especially true for DPA. The additional peaks suggest that secondary alklyamines are more reactive and/or undergo more rearrangement reactions in the ion plume than tertiary alklyamines and their corresponding reaction products.

Figure 5D shows a typical mass spectrum for particles formed from reacted DEA. A common characteristic of the DEA spectra is the presence of ion peaks at *m/z* 70, 72, and 74. This trio of peaks was also observed in the standard DEA particle mass spectra. The signal at *m/z* 86 is often the most intense and can be explained by the ion−molecule reaction

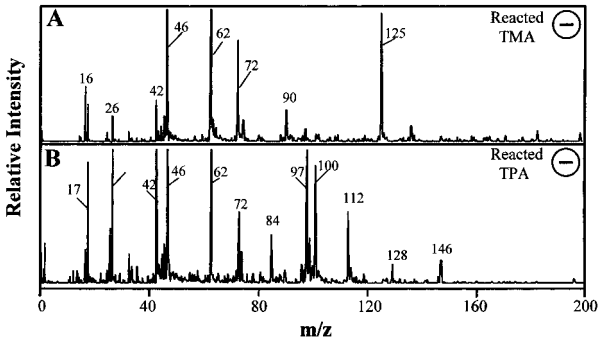

FIGURE 6. Examples of negative ion single particle mass spectra obtained from alkylamine reactions. Reactant: (A) TMA, (B) TPA. Most probable inorganic ion assignments: *m/z* 46 $[NO_2]^-$, *m/z* 62 $[NO_3]^-$, *m/z* 97 $[HSO_4]^-$, *m/z* 125 $[HNO_3NO_3]^-$. For most likely carbon-containing ion assignments, see text.

described in the section on ATOFMS mass spectral characteristics of "Alkylamine Aqueous Standard Solutions". The peaks at *m/z* 100, 101, and 102 are unique to the diethyl ammonium nitrate mass spectra and thus may be indicative of LDI plume reactions.

An example of a reacted DPA particle mass spectrum is shown in Figure 5E. As observed in the standard amine particle mass spectra, peaks occur at *m/z* 100 $[M-H]^+$, 101 $[M]^+$, and 102 $[MH]^+$. Ion signals unique to the reacted particles appear at higher *m/z* ratios, including 128, 142, and 160. Assignments are not made for these peaks because without off-line confirmation or information from previous studies, they would only be speculation. For the purposes of this paper, it is important to note that, in general, there are more high mass ion peaks observed in the particle mass spectra formed from the secondary alkylamine as compared to the tertiary alkylamine reactions. This demonstrates that secondary amines undergo different chemistry and appear to be more reactive than tertiary amines based on the relative complexity of the mass spectra.

Alkylamine Reactions−Negative Ion Mass Spectra. For all of the alkylamines studied, most of the ATOFMS signals obtained in negative polarity indicate the presence of nitrate and, less frequently, sulfate, e.g., *m/z* −42 $[CNO]^-$, −46 $[NO_2]^-$, −62 $[NO_3]^-$, −80 $[SO_3]^-$, −97 $[HSO_4]^-$, and −125 $[H(NO_3)_2]^-$ (Figure 6). Nitrate and sulfate may be present in the particle phase due to gas phase reactions between basic compounds (alkylamine and possibly their reaction products) and nitric and sulfuric acid. These acids are formed from the atmospheric oxidation of sulfur and nitrogen oxides. The possibility exists that, when filling the bag with ambient air, the HEPA filter did not completely remove all ultrafine particles with d_a below 10 nm, thus introducing sulfate and nitrate in condensed form. However, because of their small size, these particle seeds would probably not contribute significantly to the measured nitrate and sulfate ion signals. On the basis of the observed intensities, it seems more likely that nitrate and sulfate detected in the particles are the result of acid−base reactions with the alkylamines. In addition to nitrate and sulfate signals, each amine gives rise to characteristic negative ion signals. For instance, about 60% of the particle mass spectra obtained from the TMA reaction (Figure 6A) produce the *m/z* −90 signal, possibly dimethylnitramine $[CH_3N_2O_2]^-$ and, as stated previously, a positive ion signal in the corresponding positive ion mass spectrum at *m/z* 91. The signal at *m/z* −74 is most likely the fragment $[CH_3N_2O]^-$ obtained by loss of an oxygen, as opposed to dimethylnitrosamine. In fact, as indicated previously, nitrosamine should be rapidly converted to nitramine in the presence of light. However, since nitrosamines are known to be harmful to human health, the possibility of its presence in the

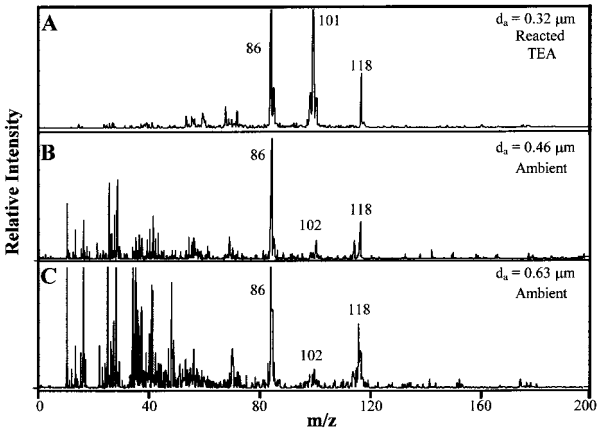

FIGURE 7. (A) Representative positive ion particle mass spectrum from the smog chamber reaction of TEA, (B) and (C) Representative positive ion mass spectra for ambient particles sampled in Riverside, CA.

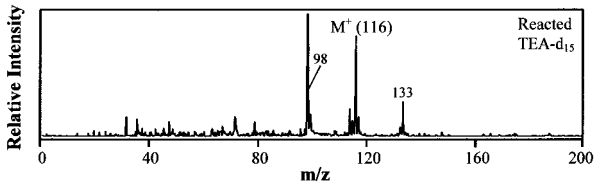

FIGURE 8. Typical positive ion single particle mass spectra obtained from deuterated triethylamine (TEA-d_{15}) reactions in smog chamber. Probable assignments for major ion peaks: *m/z* 98 $[(C_2D_5)_2N{=}CD_2]^+$, *m/z* 114 $[M-D]^+$, 116 $[M]^+$, and *m/z* 133 $[TEA\text{-}d_{15}OH]^+$.

condensed phase should be addressed in future studies. The consistent appearance of the m/z −72 signal is possibly due to $[(CH_3)_2NCO]^-$ (see Figure 6A). The reacted DEA and TEA negative ion spectra are quite simplistic, with the only organic signal found at m/z −88, which is most likely the fragment ion $[(C_2H_5)_2NO]^-$. Characteristic negative ion mass spectral signals of TPA reaction are found at m/z −128, possibly $[(C_3H_7)_2NC_2H_5]^-$, −100 $[(C_3H_7)_2N]^-$, and −72 $[(C_2H_5)_2N]^-$. These negative ion signals were not observed for the pure amine and thus are reaction products or the result of matrix effects inducing differences in plume chemistry. The m/z −146 signal is possibly due to nitramine (Figure 6B).

TEA Reaction Peak Assignments. The mass spectra of particles formed in the TEA smog chamber experiments produced the identical combination of ion peaks detected in ambient studies as shown in Figure 7. Figure 7A shows a representative spectrum for an individual particle sampled during the smog chamber reactions of triethylamine with ion peaks at m/z 86, 101, and 118. Figure 7B,C shows particles sampled in ambient air with a similar combination of ion peaks at m/z 86, 102, and 118. On the basis of the results from the standard amine and alkylammonium salt mass spectrometry studies, the peaks at 86, 101, and 102 in the particle mass spectra from the TEA reaction can be assigned to an amine fragment, most likely $[(C_2H_5)_2N{=}CH_2]^+$, TEA^+, and $TEAH^+$, respectively. However, the peak at m/z 118 observed in particle mass spectra from the triethylamine smog chamber reaction was not observed in any of the standard amine or alkyl ammonium salt spectra. Initially, it was hypothesized that the signals observed at $[M+17]^+$ for the different amines could be due to the formation of alkyl carbammic acids and/or their carbonyl-hydroxy isomers ($[CH_3NH_2COOH]^+$, $[(C_2H_5)_2NHCOOH]^+$, and $[(C_3H_7)_2NHCH_2\text{-}COOH]^+$). To test this hypothesis, an analogous smog chamber experiment was performed using fully deuterated triethylamine, TEA-d_{15}. The mass spectrum for a representative particle formed in the TEA-d_{15} reaction is shown in Figure 8. If the resulting product from the smog chamber experiment contained just 10 hydrogen atoms instead of the initial 15 (i.e., m/z 128), this would indicate carbammic acid (i.e., $[(C_2D_5)_2NHCOOH]^+$) formed in the reaction. The experimental results reveal that only approximately 4% of the particles give the corresponding peak at m/z 128. Instead, the majority of the spectra produce a signal at m/z 133, corresponding to $[M+17]^+$, in direct analogy to the product observed in undeuterated TEA reaction at m/z 118.

TABLE 2. Comparison of Mass Spectral Signals Obtained for Particles Formed in Smog Chamber Reaction of TEA and TEA-d_{15}

TEA ions, *m/z*	86	100 $(M-H)^+$	101 (M^+)	118 $(M+17)^+$
TEA-d_{15} ions, *m/z*	98	114 $(M-D)^+$	116 (M^+)	133 $(M+17)^+$
Δm	12	14	15	15

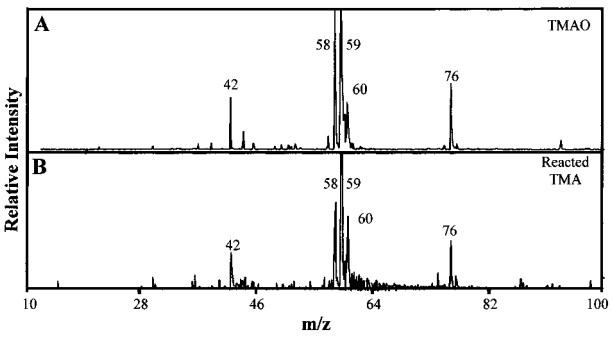

FIGURE 9. (A) Mass spectrum of a suspended solid particle of commercially acquired TMAO, and (B) Mass spectrum of reacted TMA. For ion peak assignments, see body of text.

Table 2 provides a direct comparison of the mass spectral signals obtained from reacted TEA and TEA-d_{15} particles (Figures 5B and 8), illustrating the common ion peak patterns. The assignment for the last peaks in the table at m/z 118/133, resulting from a compound containing the alkyl structure of the intact parent amine (15 H atoms), was not obvious initially. However, it has been well documented in the synthetic organic chemistry and biochemistry literature that tertiary amines can be oxidized readily through a number of different pathways to trialkylamine-*N*-oxides (*23*). This product would correspond to peaks at m/z 117 for TEA and 132 for TEA-d_{15}. However, peaks are detected at 118 and 133, indicating that these species become protonated in the LDI plume during analysis. Thus, the protonated forms of triethylamine-*N*-oxide (TEAO), trimethylamine-*N*-oxide (TMAO), and tripropylamine-*N*-oxide (TPAO) are the most probable assignments for the $[M+17]^+$ signals. Resonance structures for TEAO are shown below.

[2]

ATOFMS Mass Spectra of Trimethylamine-*N*-Oxide. To further test whether trialkylamine-*N*-oxides are formed as oxidation products of trialkylamine reactions, the mass spectral characteristics of the only commercially available alkylamine-*N*-oxide, trimethylamine-*N*-oxide, were investigated using ATOFMS. Spectra were collected for suspended solid particles, particles produced from nebulized aqueous solutions, as well as particles produced from nebulizing the same solutions acidified with nitric acid. The representative mass spectrum for a suspended solid TMAO particle is shown in Figure 9A. For all methods of generating TMAO particles, when the molecular ion is present, it occurs in the protonated

form $[MH]^+$, as indicated by the signal at m/z 76. The percentage of particles containing the $[MH]^+$ signal is larger for atomized droplets of the acidified aqueous solution (~90%) than in the other cases (~50%). Major fragments occur at m/z 58, 59, and 42, $[M\text{-}OH]^+$, $[M\text{-}O]^+$, and $[C_2H_4N]^+$, respectively. Figure 9B shows the mass spectrum from a single particle obtained in the smog chamber reactions of TMA. Comparing Figure 9A and 9B, the mass spectrum of the standard TMAO particle is identical to that obtained for particles formed upon reaction of trimethylamine. This experiment allows for the assignment of the $[M+17]^+$ ion peak at m/z 76 observed in smog chamber reactions of TMA to the protonated form of oxidized TMA, $[TMAOH]^+$. In direct analogy, these results, as well as those obtained in the TEA-d_{15} reactions, confirm the assignment of the peak at m/z 118 in particles formed in the triethylamine smog chamber reactions as $[TEAOH]^+$. By direct extension, the ion signal at m/z 118 observed in ambient particle mass spectra can be assigned to $[TEAOH]^+$. To the best of our knowledge, this is the first time oxidation products of alkylamines have been observed in the condensed phase of aerosol particles.

Control Smog Chamber Experiments. As mentioned in the Experimental Section and detailed in Table 1, a number of control experiments were performed. To confirm that particle formation is related to the presence of the amines in the Teflon bag and not due to contaminants present in ambient air, a control experiment was performed using air from our lab purification system. As expected, under these conditions, the reaction did not take place because of the absence of free radicals and nitric acid precursors. Thus, 1 ppmv CH_3ONO was added, as a source of free radicals. It must be noted that the irradiation of methylnitrite can also lead to formation of nitrogen dioxide, and in turn nitric acid (*24*). Because of the high radical concentration, particle formation occurred much faster and particles were detected by the ATOFMS after only several minutes of reaction. The mass spectra are very similar to those obtained under previous conditions. The only differences were the frequent presence of a peak at m/z 139 and, for a few particles, signals at higher masses. These peaks are not commonly observed in ambient particles, where the oxidant concentrations are lower, and thus most likely are products of further oxidation processes. Since the major focus in this study is to simulate atmospheric reactions, particle-free ambient air with natural oxidant levels was used as the reaction medium instead of clean air with higher radical concentrations from added CH_3ONO.

The same "clean" reaction has been carried out in a dry environment, with a RH of approximately 0.1% and in this case no particle formation was observed upon adding CH_3ONO. Particle formation took place instead after addition of water vapor. Most of the published literature on homogeneous particle nucleation concerns the binary system $H_2SO_4-H_2O$, and no information is available on the role of relative humidity in other nucleating systems. However, water may enter in the early nucleation process, facilitating the formation of clusters leading to stable ultrafine particles. It is also possible that water assists in the dissociation of the alkyl ammonium salts, driving the gas/particle equilibrium (i.e., partitioning) toward the particle phase over the gas phase. These preliminary results show the importance of water in alkylamine condensed phase chemistry and suggest that further experiments are necessary to fully characterize the role of water on these reaction processes.

To test the importance of sunlight irradiation for particle formation, a DEA experiment was conducted under the same conditions reported in the previous paragraph, except in the absence of light. The bag was filled with filtered ambient air, and DEA was added. The bag was stored in the dark, and the content was monitored every few hours. No particle formation was detected by the ATOFMS over a 24-h period. This can be explained by the fact that sunlight is necessary for initiating the photooxidation of the amines, as well as for producing nitric acid and thus acid−base reactions leading to alkyl ammonium salts.

Reaction Mechanism. Under typical LDI conditions, ATOFMS mass spectra often do not allow for definitive identification of the organic compounds present in the condensed phase. However, the observed signals may serve as useful indicators for some of the major constituents and thus the reaction mechanism leading to particle formation. Comparison of the data obtained in the TEA and TEA-d_{15} experiments, as well as the particle mass spectra formed from the TMAO standard and the analogous smog chamber reaction of TMA, suggest the formation of trialkylamine-*N*-oxides, species that have not been reported before for atmospheric gas or particle phase samples. The transformation of tertiary amines to the corresponding amine oxides may occur in the presence of different oxidizing agents, including peracids (*25*), hydrogen peroxide (*26*, *27*), and alkylperoxy radicals. The reaction involves a nucleophilic attack of the amine on the O−O bond. The reaction with RO_2H and H_2O_2, both less electrophilic than peracids, can be catalyzed by transition metals that may also be present in ambient particles (*28*). Other oxidation paths may involve reaction with ozone, (*29* and references therein), metal oxides (*30*), and oxygen radicals. Since all of these oxidant species are hydrophilic, they will have a tendency to partition to the aqueous phase. Thus, in ambient air, these reactions likely occur in the bulk solution of particles with high water content. This is consistent with previous ATOFMS field studies where a strong RH dependence of the amine-related peaks at m/z 86, 101, 102, and 118 in ambient particle mass spectra has been observed (i.e., Figures 1 and 2).

TMAO and TEAO are used in many industrial processes (*31*, *32*) and widely diffuse in living organisms, playing a central role in many biological oxidative reactions (*33*, *34*). Therefore, while these compounds form in the smog chamber from trialkylamine photooxidation processes, it is also possible they may be emitted directly into the environment in their oxidized forms.

Particle Formation. Short alkyl chain aliphatic amines have relatively high vapor pressures, and thus when present in the particle phase, they most likely occur in the form of alkyl ammonium salts. The fact that most of the negative ion spectra contain peaks due to nitrates is consistent with this hypothesis. If water is present in these particles, the salts will dissolve into their ionic forms, thereby removing these compounds from the gas phase. This will result in an equilibrium shift from the gas phase to the particle phase for these species. The observed diurnal behavior suggests they are semivolatile. This study demonstrates the potential for using ATOFMS as a monitor for semivolatile species in the atmosphere, characterizing the short-term variations of individual organic species over time.

Because gas-to-nitrate particle conversion and gas phase amine photooxidation processes are known from previous studies to be rapid reactions, the relatively long time required to observe particles with the ATOFMS in the smog chamber experiments can most likely be attributed to the time required for the particles to grow up to the ATOFMS size detection limit, e.g., $d_a > 0.2\ \mu m$. On the other hand, in ambient air, clusters of the products (i.e., alkyl ammonium salts, alkylamine oxide, and other reaction products) may coagulate onto preexisting particles. This was tested by introducing ambient particles in the smog chamber at the end of the TEA experiment. After several minutes, nearly all of the particle mass spectra analyzed showed the general amine marker ion at m/z 86, as well as peaks at m/z 101, 102, 118 and typical ambient organic and inorganic ion signals. Overall,

the ATOFMS mass spectra obtained from acid-amine reactions in the presence of these ambient particles are even more similar to those observed in ambient air than the spectra obtained from the reactions of pure amines.

The experiments performed in this study demonstrate that particle formation occurs in the presence of short alkyl chain secondary and tertiary amines in a smog chamber, producing particles with mass spectra that are very similar to those observed for particles in the atmosphere. The combination of experiments performed in this study illustrates how mass spectral markers can assist in the identification of species in ambient particles. As described, particles containing these markers are very commonly observed and possible sources include the large cattle feedlots in the nearby city of Chino, CA, as well as vehicle exhaust based on ATOFMS source characterization and roadside studies (*16*). In looking through the patent literature, a possible source for the amines in mobile emissions may be additives and/or detergents. These results suggest that photooxidation and gas-to-particle reaction processes of amines could be significant contributors to ambient particles and should be considered in atmospheric chemistry models. More extensive analysis of ambient data from past field campaigns, in light of the findings in these studies, will provide a means to improve our knowledge of the condensed-phase chemistry of alkylamines.

Acknowledgments

The authors gratefully acknowledge Professors Paul Ziemann, Roger Atkinson, Janet Arey, and Thomas Morton for helpful discussions. Also, the authors thank Dr. Don Liu and Ryan Wenzel for the Atlanta data used in Figure 2. Financial support for this research was provided by the National Science Foundation (CHE-9412317), the California Air Resources Board (Contract 95-305), and the National Renewable Energy Laboratory (ACI-8-17075-01).

Literature Cited

(1) Finlayson-Pitts, B. J.; Pitts, J. N., Jr. In *Atmospheric Chemistry*; Wiley-Interscience: New York, 1986.
(2) Cadle, S. H.; Mulawa, P. A. *Environ. Sci. Technol.* **1980**, *14*, 718.
(3) Westerholm, R.; Li, H.; Almen, J. *Chemosphere*, **1993**, *27*, 1381.
(4) Mosier, A. R.; Andre, C. E.; Viets, F. G., Jr. *Environ. Sci. Technol.* **1973**, *7*, 642.
(5) Schade, G. W.; Crutzen, P. J. J. *Atmos. Chem.* **1995**, *22*, 319.
(6) Manahan, S. E. *Environmental Chemistry*, 4th ed.; Lewis, 1990.
(7) Shapley, D. *Science* **1976**, *191*, 269.
(8) Fine, D. H.; Rounbehler, D. P.; Belcher, N. M.; Epstein, S. S. *Science* **1976**, *192*, 1328.
(9) Pitts, J. N., Jr.; Grosjean, D.; Van Cauwenberghe, K.; Schmid, J. P.; Fitz, D. R. *Environ. Sci. Technol.* **1978**, *12*, 946.
(10) Hanst, P. L.; Spence, J. W.; Miller, M. *Environ. Sci. Technol.* **1977**, *11*, 403.
(11) Finlayson-Pitts, B. J.; Pitts, J. N., Jr. *Chemistry of the Upper and Lower Atmosphere*; Academic Press: 2000.
(12) Suess, D. T.; Prather, K. A. *Chem. Rev.* **1999**, *99*, 3007.
(13) Prather, K. A.; Nordmeyer, T.; Salt, K. *Anal. Chem.* **1994**, *66*, 1403.
(14) Nordmeyer, T.; Prather, K. A. *Anal. Chem.*, **1994**, *66*, 3540.
(15) Gard, E.; Mayer, J. E.; Morrical, B. D.; Dienes, T.; Fergenson, D. P.; Prather, K. A. *Anal. Chem.* **1997**, *69*, 4083.
(16) Suess, D. T., Silva, P., Gross, D., Schauer, J., Cass, G., Prather, K., submitted to *Environ. Sci. Technol.* **2001**.
(17) Russell, Armistead G.; McRae, Gregory J.; Cass, Glen R. *Atmos. Environ.* **1983**, *17*, 949.
(18) McLafferty, F. W.; Turecek, F. Interpretation of Mass Spectra; 4th ed.; University Science Books: Sausalito, CA, 1993.
(19) Silva, P. J.; Prather, K. A. *Anal. Chem.* **2000**, *72*, 3553.
(20) Haas, Y.: Lifshitz, C. *Chem. Phys. Lett.* **1983**, *97 (4−5)*, 467−470.
(21) Moritz, F.; Grotemeyer, J. *J. Org. Mass Spectrom.* **1993**, *28*, 207.
(22) Chou, J. S.; Sumida, D.; Wittig, C. *Chem. Phys. Lett.* **1983**, *100*, 209.
(23) Sauer, J. D. *Cationic Surfactants: Organic Chemistry*, Vol. 34; Richmond, J. M., Ed.; Marcel Dekker: New York, 1990.
(24) Atkinson, R., Aschmann, S. M., Pitts, J. N., Jr., *Environ. Sci. Technol.* **1984**, *18*, 110−113.
(25) Plesnièar, B. *Organic Chemistry*, Part C, Trahanovsky W. S., Ed., Academic Press: New York, 1978.
(26) Lewis, S. N. in *Oxidation: Techniques & Applications in Organic Synthesis*, Vol. 1, Augustine R. L., Ed.; Marcel Dekker: New York, 1969−1971.
(27) Suresh, S.; Joseph, R.; Jayachandran, B.; Pol, A. V.; Vinod, M. P.; Sudalai, A.; Sonawane, H. R.; Ravindranathan, T. *Tetrahedron* **1995**, *51*, 11305.
(28) Sheldon, R. A., Kochi, J. K. In *Metal-Catalyzed Oxidation of Organic Compounds*. Academic Press: New York, 1981.
(29) Bailey, P. S.; Carter, T. P.; Jr., Southwick, L. M. *J. Org. Chem.* **1972**, *37*, 2997.
(30) Rousselet, G.; Capdevielle, P.; Maumy, M. *Tetrahedron Lett.* **1995**, *36*, 4999.
(31) Knolker, H. J. Prakt. *Chemie-Chemiker-Zeitung* **1996**, *338*, 190.
(32) Akesson, B., Vinge, E., Skerfving, S. *Toxicol. Appl. Pharmacol.* **1989**, *100*, 529.
(33) Horiuchi, M.; Umano, K.; Shibamoto, T. *J. Agric. Food Chem.* **1998**, *46*, 5232.
(34) Sadok, S.; Uglow, R. F.; Haswell, S. J. *Anal. Chim. Acta* **1996**, *334*, 279.

Received for review August 2, 2000. Revised manuscript received April 25, 2001. Accepted April 30, 2001.

ES0015444